

УДК 538.9

N.V. Shevchenko, G. Gershteyn, M. Schaper, Fr.-W. Bach

## STRUCTURE INVESTIGATION OF AUSTENITIC STEEL AFTER COLD ROLLING DEFORMATION

*Transmission electron-microscopic investigations of the austenitic steel 316L and a TWIP steel after cold rolling and tensile plastic deformation at room temperature was carried out. It is shown that the basic deformation mechanisms are sliding dislocation, twinning and shear band formation. Possible conditions of forming mechanisms specified above are discussed.*

*Keywords: austenitic steel; cold rolling; twins; shear bands; TEM.*

*Проведено електронно-мікроскопічне дослідження аустенітної сталі після пластичної деформації прокаткою і розтягуванням при кімнатній температурі. Показано, що основними механізмами деформації є дислокаційне сколювання, двійниковання та утворення смуг локалізації деформації. Обговорюються можливі механізми формування зазначених вище станів.*

*Ключевые слова: аустенитная сталь, холодная прокатка, двойникование, локализованные полосы сколювания, ПЭМ.*

*Проведено електронно-мікроскопічне дослідження аустенітної сталі після пластичної деформації прокаткою і розтягуванням при кімнатній температурі. Показано, що основними механізмами деформації є дислокаційне ковзання, двійниковання та утворення смуг ковзання, які локалізовані. Обговорюються можливі механізми формування зазначених вище станів.*

*Ключові слова: аустенітна сталь, холодна прокатка, двійниковання, смуги локалізації деформації, ПЕМ.*

### Introduction

Severe plastic deformation (SPD) which occurs during technological processes like rolling leads to a submicro- and nanostructuring of materials. Knowledge of the physical laws and mechanisms of the plastic deformation at a high degree of deformation enable an improved processing. Due to the rotating material flow and the formation of shear bands during SPD different kinds of material structure will occur. Knowledge of the formation mechanism of the material structures allows the simulation of the forming process. Thereby, the classification of the material structures enables to parameterize the simulation. The aim of this work is to investigate the formation mechanism of the material structures of austenitic steels during rolling and tensile tests.

### Experimental procedure

For the research the alloyed steel 316L (Fe; 16.8 %Cr; 14.1 %Ni; 1 %Mn; 2.1 %Mo; 0.01 %N; 0.007 %C; 0.04 %Si) and a TWIP-steel (Mn < 24 %; C < 1.0 %; Al < 3 %; Si < 3%) were used.

Prior to their deformation, the specimens were recrystallized for one hour at 1100 °C. The steels were plastically deformed by rolling at room temperature to deformation values  $\varepsilon$  in the range from 10 % to 70 %.

Subsequent to the deformation, TEM specimens were prepared. The specimens with a diameter of 3 mm were extracted perpendicular to the rolling direction and finely grounded and polished until achieving thin sections with a thickness of approximately 100  $\mu\text{m}$  and a surface roughness of  $R_a < 1 \mu\text{m}$ . The 316L steel TEM foils were electropolished in an electrolytic solution composed of 450 ml orthophosphoric acid, 50 g chromium trioxide and 2 ml hydrogen peroxide; the TWIP steel foils were electropolished in the Elektrolyt A2, using a TenuPol 5 (made by the company Struers) with a current density of 100 mA/cmI. The microstructure and phase compositions were investigated by means of a JEOL JEM-2010 transmission electron microscope.

### Results

The transmission electron microscopic investigations carried out on the 316L steel showed that a high dislocation density already exists in the initial state.

Figure 1 shows a typical microstructure for the 316L steel after recrystallisation. One can discern a non-uniform distribution of straight and curved dislocations, accumulations of dislocations and stacking faults. Above all, some grains contain isolated annealing twins in the size of 1  $\mu\text{m}$  to 10  $\mu\text{m}$ . An estimate of the dislocation density  $\rho$  yields about  $10^9 \text{ cm}^{-2}$ . It is well known that this dislocation density increases with increasing the degree of deformation. Moreover, as already described in [1, 3 and 4] for fcc materials, one observes the substructures as cellular formations.

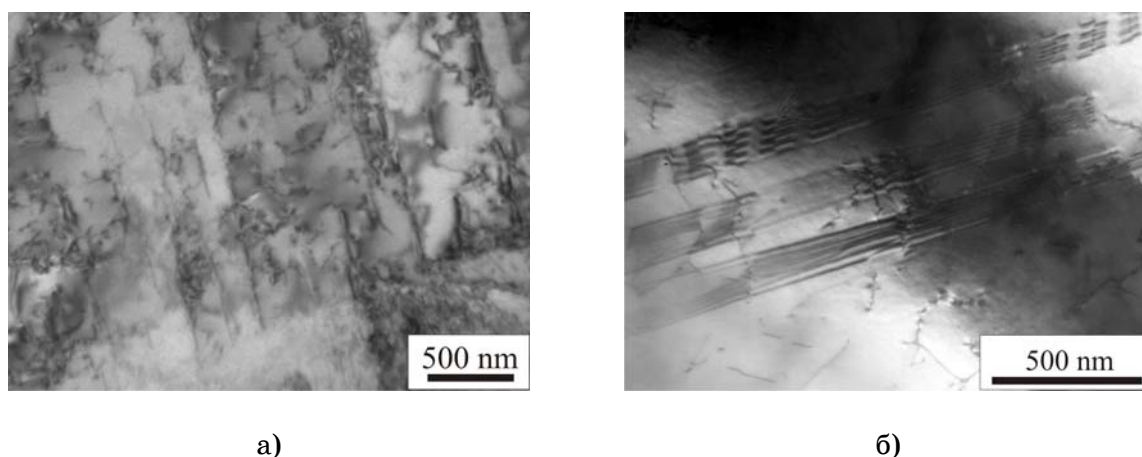


Figure 1 - Microstructure of the 316L steel in the initial state. Bright-field of the dislocation structure (a) and stacking-faults (b)

A similar structure can also be discerned in the TWIP-steel's initial state (figure 2). The grain size depicted here is approximately 10  $\mu\text{m}$ . Within the grain, one can observe random distributions of dislocations, dislocation groups

and stacking faults. The dislocation density is about  $10^9 \text{ cm}^{-2}$ . Furthermore, annealing twins having dimensions of tenths of micrometers can be detected within the grains.

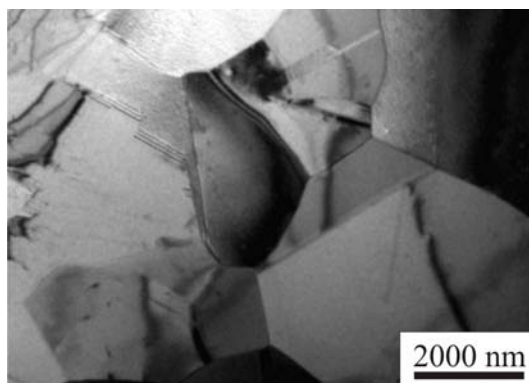


Figure 2 - Initial microstructure of the investigated TWIP steel

After a deformation  $\varepsilon$  of 30 % by rolling, one detects mixed types of substructures in the 316L (figure 3). Here, the fraction of material which is occupied by twin structures is comparatively small. Mechanical twinning is observed not only in this system but also in those of neighbouring systems. An estimate of the dislocation density yields  $10^{10} \text{ cm}^{-2}$ . Thus, subsequent to a given level of plastic deformation, the formation of twin structures and dislocation glide are the competing deformation mechanisms.

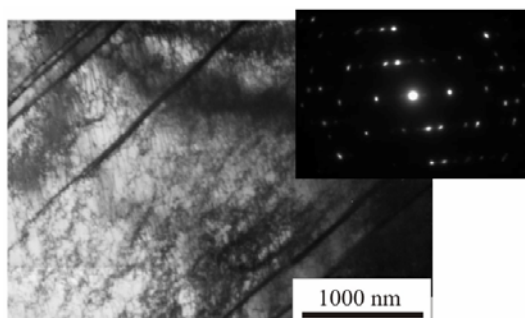


Figure 3 - Bright-field image and diffraction pattern of the mixed type of substructures following rolling to a true strain of  $\varepsilon \sim 30 \%$

On raising the deformation to  $\varepsilon \sim 50 \%$ , the influence of the mechanical twinning significantly increases. In figure 4 the microtwinning structures are depicted, which have formed as a consequence of deforming 316L steel to a strain  $\varepsilon$  of 50 %. The fraction of the material which is occupied by twin structures, significantly increases, whereas the cellular substructure in the material's lower layer was not observed. The TEM analysis revealed that the twins (figure 4) are approximately several tens of nanometers thick.

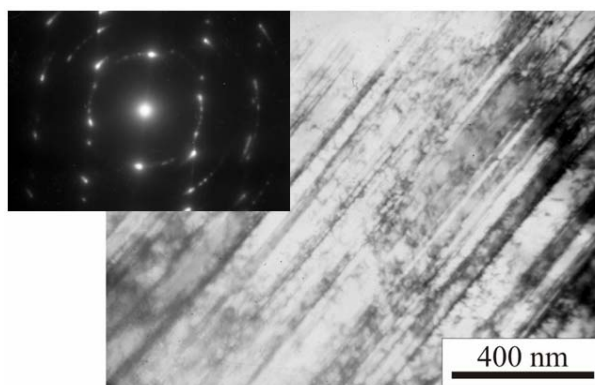


Figure 4 - Deformation of microtwins in the steel 316L subsequent to rolling to a true strain of  $\varepsilon \sim 50 \%$

The twins previously formed during deformation tend to invert in the course of additional deformation processes. As a rule, according to [3] this occurs with twins, which exist in favourably oriented grains, being translated in a plane which lies parallel to the rolling plane.

The investigations show that, following a deformation of  $\varepsilon \sim 50 \%$ , a predominant portion of the microtwin packets either lie parallel to or deviate by only a small angle from the rolling plane. Here, twin formation can be observed in a few grains in which the twin planes intersect. Subsequent to increasing the deformation to  $\varepsilon \sim 70 \%$  (figure 5), and in contrast to twin formation [4, 5], the regions adopt another structure in the form of localised shear bands.

The micro bands' common features are:

- Non-crystallographic slip; that is, the micro bands do not lie on slip planes;
- The width of the formed bands are in the micrometer range;
- The lengths are in the range of tenths of micrometers;
- The bands have developed an internally fragmented structure.

One such shear band can be seen in Figure 6

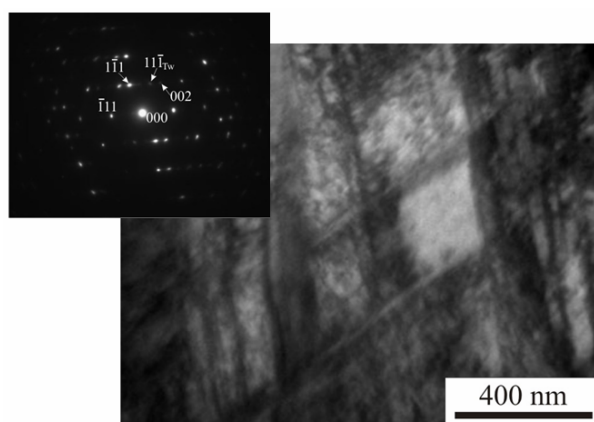


Figure 5 - Intersection of two microtwin systems following rolling to a deformation  $\varepsilon$  of about 70 %; bright-field image with diffraction pattern of the microtwin systems

As figure 6 makes clear, the localised deformation shear band extends into the microtwin's structure. The thickness of the microtwins is 10 nm to 100 nm. Within the shear band, a fragmented substructure is developed. The fragments are of the size of 10 nm to 100 nm. The main mechanism of substructure formation changes with increasing deformation.

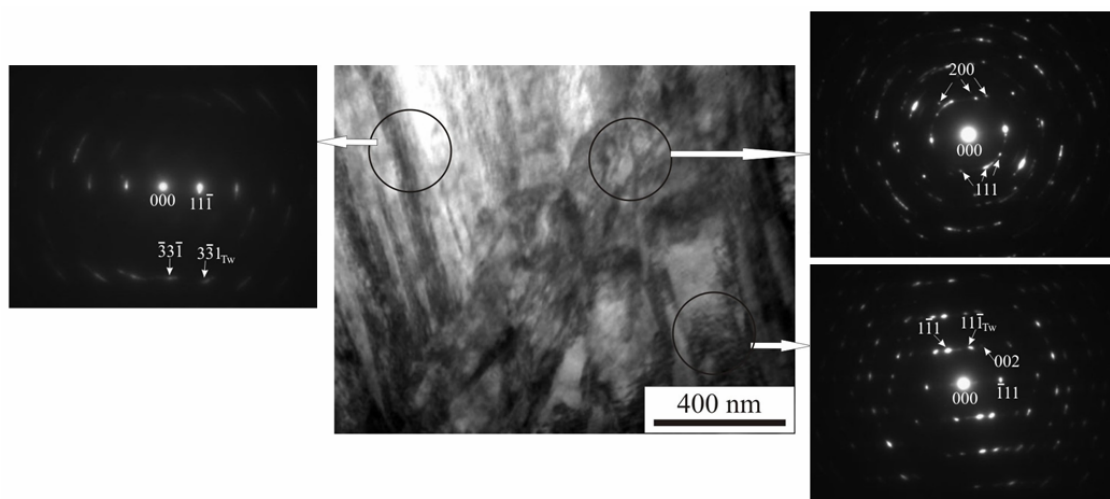


Figure 6 - Shear band in 316L steel following rolling to a deformation  $\varepsilon \sim 70\%$ . Bright-field image depicting a shear band and its surrounding region; diffraction pattern of the localised shear band and of the deformation twins corresponding to the regions above and below the shear band

This is characterised by the formation of localised shear bands due to the "saturation" level of twinning. The shear bands' frequency of occurrence in the material increases with the degree of deformation. In this way, the dimensions of the fragments decrease and form the slip-bands' internal structure. Thus, the complex interactions which occur between the shear bands, the twin structures and shear bands of other systems lead to a continuous increase in the fraction of the fragmented structure

The investigation of the TWIP steel also shows system non-specific twinning between two or more systems following a deformation of  $\varepsilon \sim 50\%$  [6, 7]. Figure 7 shows a localised shear band and clearly illustrates the internally fragmented structure which extends into the microtwin structure.

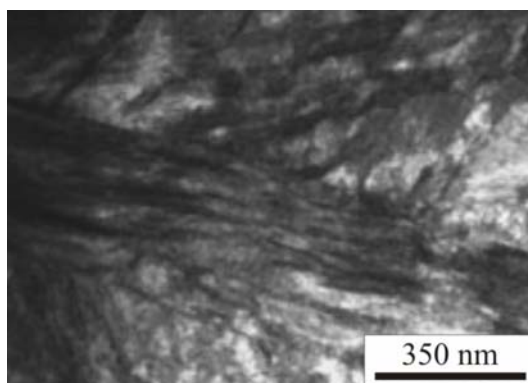


Figure 7 - A localised shear band in the TWIP steel and the surrounding microtwins following an applied deformation of up to  $\varepsilon \sim 50\%$

It is assumed that the influence of the different amounts of alloying elements in TWIP steel, compared to those in the 316L steel, caused the formation of localised shear bands.

### Summary

The TEM investigations demonstrated that mechanical twinning and the formation of localised deformation shear bands are the most important mechanisms for forming substructures in austenitic steels. These mechanisms are caused by plastic deformation during rolling at room temperature.

The mechanism of twinning dominates at low true strain levels but is replaced by the formation of locally deformed shear bands with increasing deformations. As a consequence a complex interaction between the microtwins and the locally deformed shear bands occurs.

By investigating and analysing the deformation patterns, information can be obtained that allows developing specifically adjusted microstructures which possess defined mechanical properties.

Moreover, it can be assumed that an analysis of changes in deformation patterns and plastic deformation mechanisms leads to the knowledge to form of nanostructural states.

### Acknowledgements

The presented investigations were carried out within the framework of the project cluster (PAK250) "Identification and modelling of material characteristics for the Finite Element Analysis of sheet forming processes" in the sub project TP5 supported by German Research Foundation (DFG). The authors would like to thank the DFG for the granted support. This work was made possible for the Institute of Strength Physics and Material Science SB RAS by the Russian Federation through the financial support MK-2909.2009.8.

### LITERATURE

1. Wang H.S., Wei R.C., Huang C.Y., Yang J.R. Cross-sectional transmission electron microscopy of ultra-fine wires of AISI 316L stainless steel // Phil. Mag., Vol. 86, 2006, pp. 237 – 251.

2. Liao X.Z., Zhou F., Lavernia E.J. et al. Deformation mechanism in nanocrystalline Al: Partial dislocation slip // *Appl. Phys. Lett.*, 83, 2003, pp. 632 – 634.
3. Donadille C., Valle R., Dervin P., Penelle R. Development of texture and micro structure during cold - rolling and annealing of FCC alloys: example of an austenitic stainless steel // *Acta metal.*, 37, 1989, pp. 1547 – 1571.
4. Meyers M.A., Xu Y.B., Xue Q. et al. Microstructural evolution in adiabatic shear localization in stainless steel // *Acta Mat.*, Vol. 51, 2003, p. 1307 – 1325.
5. Morikawa T., Higashida K., Sato T. Fine-grained structures developed along grain boundaries in a cold-rolled austenitic stainless steel // *ISIJ International.*, Vol. 42, 2002, pp. 1527 – 1533.
6. Vercammen S., Blanpain B., De Cooman B.C., Wollants P. Cold rolling behaviour of an austenitic Fe-30Mn-3Al-3Si TWIP-steel: the importance of deformation twinning // *Acta Mat.* Vol. 52, 2004, pp. 2005 – 2012.
7. Hua Ding, Zheng-You Tang, Wei Li, Mei Wang, Dan Song. Microstructures and Mechanical Properties of Fe-Mn-(Al, Si) TRIP/TWIP Steels // *Journal of Iron and Steel Research, Int.*, Vol. 13, 2006, pp. 66 – 70.